THE JOURNAL OF BIOLOGICAL CHEMISTRY
Vol. 276, No. 13, Issue of March 30, pp. 10153–10160, 2001

Printed in U.S.A.

The Human $VPAC_1$ Receptor

THREE-DIMENSIONAL MODEL AND MUTAGENESIS OF THE N-TERMINAL DOMAIN*

Received for publication, October 25, 2000, and in revised form, December 21, 2000
Published, JBC Papers in Press, December 21, 2000, DOI 10.1074/jbc.M009730200

Laurence Lins‡§, Alain Couvineau‡§, Christiane Rouyer-Fessard‡, Pascal Nicole‡¶, Jean-José Maoret‡, Moussa Benhamed‡, Robert Brasseur‖, Annick Thomas‡, and Marc Laburthe‡ ‡‡**

From ‡Unité INSERM U410 de Neuroendocrinologie et Biologie Cellulaire Digestives, Institut National de la Santé et de la Recherche Médicale, Faculté de Médecine Xavier Bichat, Paris F-75018, France and the ‖Centre de Biophysique Moléculaire Numérique, Faculté Universitaire de Gembloux, Gembloux B-5030, Belgium

The human $VPAC_1$ receptor for vasoactive intestinal peptide (VIP) and pituitary adenylate cyclase activating peptide belongs to the class II family of G-protein-coupled receptors with seven transmembrane segments. Like for all class II receptors, the extracellular N-terminal domain of the human $VPAC_1$ receptor plays a predominant role in peptide ligand recognition. To determine the three-dimensional structure of this N-terminal domain (residues 1–144), the Protein Data Bank (PDB) was screened for a homologous protein. A subdomain of yeast lipase B was found to have 27% sequence identity and 50% sequence homology with the N-terminal domain (8–117) of the $VPAC_1$ receptor together with a good alignment of the hydrophobic clusters. A model of the N-terminal domain of $VPAC_1$ receptor was thus constructed by homology. It indicated the presence of a putative signal sequence in the N-terminal extremity. Moreover, residues (Glu^{36}, Trp^{67}, Asp^{68}, Trp^{73}, and Gly^{109}) which were shown to be crucial for VIP binding are gathered around a groove that is essentially negatively charged. New putatively important residues for VIP binding were suggested from the model analysis. Site-directed mutagenesis and stable transfection of mutants in CHO cells indicated that Pro^{74}, Pro^{87}, Phe^{90}, and Trp^{110} are indeed important for VIP binding and activation of adenylyl cyclase activation. Combination of molecular modeling and directed mutagenesis provided the first partial three-dimensional structure of a VIP-binding domain, constituted of an electronegative groove with an outspanning tryptophan shell at one end, in the N-terminal extracellular region of the human $VPAC_1$ receptor.

The $VPAC_1$ receptor for the neuropeptides vasoactive intestinal peptide (VIP)[1] and pituitary adenylate cyclase activating peptide is a class II G protein-coupled receptor (1). Together with the $VPAC_2$ receptor subtype, they mediate a large array of VIP or pituitary adenylate cyclase activating peptide actions on exocrine secretions, release of hormones, relaxation of muscles, metabolism, growth control of fetuses, and tumor cells and embryonic brain development (2, 3). Class II receptors for peptides have low sequence homologies with other members of the superfamily of G protein-coupled receptors (1, 4). They share several specific properties, the most important of which is the presence of large N-terminal extracellular domains which contain 10 highly conserved amino acids including six cysteines, putative N-terminal leader sequences and several potential *N*-glycosylation sites (1, 4–6). A complex gene organization with many introns is also common to all class II receptors (5). We know from mutagenesis studies that the N-terminal extracellular domain plays a dominant, although not exclusive, role in determining the peptide ligand binding affinity (1, 4–6). However, no structure of the large N-terminal extracellular domain of the class II receptors is yet available.

The human $VPAC_1$ receptor has been extensively characterized by site-directed mutagenesis and construction of receptor chimeras (7–14). The data demonstrate an important role of the N-terminal extracellular domain constituted of 144 amino acid residues: in this fragment, Glu^{36}, Trp^{67}, Asp^{68}, $Tryp^{73}$, Gly^{109}, and Lys^{143} are crucial for VIP binding affinity (7, 10, 11, 13); six cysteines are required to ensure VIP binding (8); two (Asn^{58} or Asn^{69}) out of the three *N*-glycosylation sites play a mandatory role for correct delivery of the receptor to the plasma membrane (9). Other domains that are functional for VIP binding (8, 14) or peptide selectivity (13) have been mapped in extracellular loops and in the third transmembrane domain of human $VPAC_1$ receptor. Recently, constitutively active mutants of human $VPAC_1$ receptor have been produced after point mutagenesis of Arg (15) or Thr (16) residues of the second and fourth transmembrane domain, respectively.

The residues (Glu^{36}, Trp^{67}, Asp^{68}, Trp^{73}, Gly^{109}, and Lys^{143}) which are crucial for VIP binding affinity are dispersed along the primary sequence of the N-terminal extracellular region of the human $VPAC_1$ receptor. We question whether their spatial distribution is responsible for their functional properties. In this paper, we have developed the first threee-dimensional model of a large part of the N-terminal domain of the human

* This work was supported by the Institut National de la Santé et de la Recherche Médicale (INSERM), the "Interuniversity Poles of Attraction Program-Belgian State, Prime Minister's Office-Federal Office for Scientific, Technical and Cultural Affairs" contract number P.4/03, the Loterie Nationale, and the National Fund for Scientific Research of Belgium. The costs of publication of this article were defrayed in part by the payment of page charges. This article must therefore be hereby marked "*advertisement*" in accordance with 18 U.S.C. Section 1734 solely to indicate this fact.

§ Contributed equally to the results of this work.
¶ Ph.D. student at the University Paris 11.
** Research Director at the National Funds for Scientific Research of Belgium.
‡‡ Director of Research at the Center National de la Recherche Scientifique (CNRS). To whom correspondence should be addressed: INSERM U410, Faculté de Médecine Xavier Bichat, 75018 Paris, France. Tel.: 33-1-44-85-61-30; Fax: 33-1-44-85-61-24; E-mail: laburthe@bichat.inserm.fr.

[1] The abbreviations used are: VIP, vasoactive intestinal peptide; GFP, green fluorescent protein; VPAC receptor (for official nomenclature, see Ref. 8); CHO, Chinese hamster ovary cells; HCA, hydrophobic cluster analysis.

VPAC$_1$ receptor by homology modeling. Although the already available data from site-directed mutagenesis experiments (7, 11, 13) were not used as modeling constraints, the structure obtained does accommodate them and generates new hypotheses regarding the possible role of several amino acid residues. Hypotheses were experimentally tested by mutagenesis. Altogether, molecular modeling and mutagenesis suggest that an electronegative groove topped at one end by a tryptophan shell could constitute a partial VIP-binding domain in the human VPAC$_1$ receptor.

EXPERIMENTAL PROCEDURES

Materials—Enzymes and vectors were obtained from Promega (Charbonnière, France) and culture medium from Life Technologies, Inc. (Cergy-Pontoise, France). Synthetic VIP was from Neosystem (Strasbourg, France). ^{125}I-VIP was prepared and purified as described (17). Other highly purified chemicals used were from Sigma (Saint-Quentin-Fallavier, France).

Molecular Modeling—A three-dimensional model of the 1–144 N-terminal domain of the human VPAC$_1$ receptor was calculated using the Modeller 4.0 software (18, 19). This method uses sequence homology between the receptor protein domain and a protein whose three-dimensional structure is known to predict a three-dimensional model. To find an homologous sequence to the VPAC$_1$ receptor 1–144 sequence, we screened the Protein Data Bank using the FASTA algorithm (20). The 152–262 region of a yeast lipase was selected (Protein Data Bank code: 1LBS), carrying 27% sequence identity and 50% sequence homology with residues 8–117 of the VPAC$_1$ receptor. To further check the homology, the HCA (hydrophobic cluster analysis) plots of both sequences were compared using the Visualfasta program (Patrick Durand, Paris, France). Briefly, the HCA method is based on a two-dimensional helical plot of the sequence, allowing detection of hydrophobic clusters in proteins (21). Alignment of hydrophobic clusters mostly supports homologous folds. The quality of alignment is evaluated by the HCA score. In this case, the score is 60%. The resulting alignment is used as input for Modeller 4.0. The three-dimensional structure d1 calculated by Modeller4 is then minimized using the Hyperchem 5.0 software (Hypercube Inc.). The energy minimization is carried out using the conjugate gradient method with the AMBER forcefield. The stereochemical quality of the minimized three-dimensional model is finally checked using Procheck (22). The model has 88% of the Φ,Ψ angle pairs in the allowed regions of the Ramachandran plot, indicating a correct stereochemistry. Electrostatic potentials were calculated and drawn using CHIME (MDL Information system Inc.). Molecular views were drawn with the WinMGM program (23).

Site-directed Mutagenesis Experiments—Oligonucleotide-directed mutagenesis was performed as previously described (4). Identification of the desired mutations was obtained by direct double-stranded sequencing of the mutated region (7). To control the correct expression of the wild-type and mutated VPAC$_1$ receptor in transfected cells, each construction was fused in the C-terminal position with the green fluorescent protein (GFP) in the eukaryote expression vector pEGFP-N2 (CLONTECH, Palo Alto, CA) as described (11). We previously demonstrated that the presence of GFP at the C terminus of VPAC$_1$ receptor does not modify its phenotype with respect to VIP binding and activation of adenylyl cyclase (11). For mutants with null phenotypes, new constructs were developed in which a Flag sequence was inserted after the leader peptide between Ala^{30} and Ala^{31} as described (15). It was previously shown that this insertion does not modify the dissociation constant for VIP or the dose response of VIP in stimulating cAMP production as compared with the native VPAC$_1$ receptor (15). This extracellular Flag made it possible to directly assess the cell surface expression of mutated receptors (15) by immunofluorescence and anti-Flag antibody binding experiments (see below).

Cell Transfection—Wild-type and mutated VPAC$_1$ receptors were stably transfected into CHO cells as previously described (25) using 3 μl of Fugen-6 (Life Technologies, Cergy-Pontoise, France) and 2 μg of DNA construct. After transfection and 48 h of culture, GFP fluorescence was observed to estimate receptor expression as previously reported (11). CHO cells were selected in the presence of geneticin (G418) at a final concentration of 0.8 g/liter for 4 days, then they were grown for 3–4 days without G418. After a second round of G418 selection (0.8 g/liter) for 4 days, CHO cells were grown without G418 and used for fluorescence studies (see below) or for membrane preparation as described (7).

Ligand Binding Assay and Measurement of Adenylyl Cyclase Activity—The binding properties of the wild-type and mutated VPAC$_1$ receptors were analyzed by competitive inhibition of ^{125}I-VIP binding to transfected cell membranes by unlabeled VIP as previously described (17). Binding parameters (K_d and B_{max}) were determined using the LIGAND computer program (26). Adenylyl cyclase activity was assayed as previously reported (27). Each experiment consisted of a full concentration-response curve and the concentration of VIP which induced half-maximal response (EC_{50}) was determined. Protein content in membrane preparations was evaluated by the procedure of Bradford (28) using bovine serum albumin as standard.

Fluorescence Studies—Microscopy immunofluorescence studies on transfected CHO cells were performed on nonpermeabilized cells using anti-Flag antibodies as described (15). Briefly, transfected cell suspensions are incubated with the mouse monoclonal anti-Flag antibodies diluted in phosphate-buffered saline containing 1% (w/v) bovine serum albumin, washed, and then incubated with anti-mouse immunoglobulin G conjugated to rhodamine. Cells are then collected directly on microscope slides by centrifugation at 700 rpm for 10 min (Cytospin3, Shandon Pittsburgh PA) and selected fields are observed using a Leica DM IRB microscope. The fluorescence of GFP in stably transfected living cells was observed directly on a Leica DM IRB microscope. All images were obtained and treated with the Archimed Pro software (Micromécanique, Evry, France).

Assessment of Cell Surface Expression of Mutated Receptors—Cell surface expression of mutated receptors with null phenotypes was assessed using the mouse monoclonal anti-Flag antibodies as described (15) with minor modifications. Briefly, transfected cells were incubated with anti-Flag antibodies diluted in phosphate-buffered saline containing 1% (w/v) bovine serum albumin, then washed and incubated in presence of the radiolabeled second antibodies (^{125}I-labeled goat anti-mouse whole IgG). The radioactivity was determined in cell lysates. Nonspecific binding was determined with cells only incubated with radiolabeled second antibodies. Binding of anti-Flag antibodies to epitope-tagged mutant receptors was given as a percentage of specific anti-Flag antibodies binding to epitope-tagged wild type receptor (15).

RESULTS AND DISCUSSION

The N-terminal domain of the VPAC$_1$ receptor is isolated from the rest of the protein in the extracellular medium. It has a predicted length of 144 residues (24) and thus is large enough to be folded as an independent domain (29). We looked for a protein sharing sequence homology with the N-terminal sequence of the VPAC$_1$ receptor in the Protein Data Bank that contains proteins with known three-dimensional structures. Using the FASTA algorithm (20), the 152–262 fragment of *Candida antarctica* yeast lipase B (PDB code 1LBS) was selected. This region is a subdomain of the lipase with a self fold. It shares 27% sequence identity and 50% sequence homology with the 8–117 region of the VPAC$_1$ receptor (Fig. 1*A*) which will be referred to as VPAC$_1$-(8–117), the sequence homology and identity, the good alignment of hydrophobic clusters, and the similar distribution of proline and glycine residues validate the calculation of a three-dimensional model of the 8–117 region of the VPAC$_1$ receptor based on the crystal structure of the *C. antarctica* yeast lipase B.

A three-dimensional model of VPAC$_1$-(8–117) was therefore built using Modeller 4.0 (18, 19), refined by energy minimization, and validated by Procheck (22) (Fig. 2, *A* and *B*). The local root mean square distance between the VPAC$_1$-(8–117) three-dimensional model obtained and the lipase subdomain is 3.8 Å, indicating a very similar fold of the two protein subdomains. This is illustrated in Fig. 2 which shows a three-dimensional image of the lipase structure *versus* the three-dimensional model of VPAC$_1$-(8–117). The VPAC$_1$-(8–117) structure shows an overall good compactness, except for the N-terminal extremity (residues 8–30) which looks as a separated, mostly helical structure (Fig. 2*B*). This fragment was previously hypothesized to be a signal peptide (24). The model agrees with and even reinforces the suggestion. Furthermore, the hydrophobicity of the 11–23 fragment is sufficient to support an interaction with a membrane and furthermore, the structure is mobile around the loop located at residues 24–28. The main secondary structure of the 8–117 model is coil since the α helix percentage is

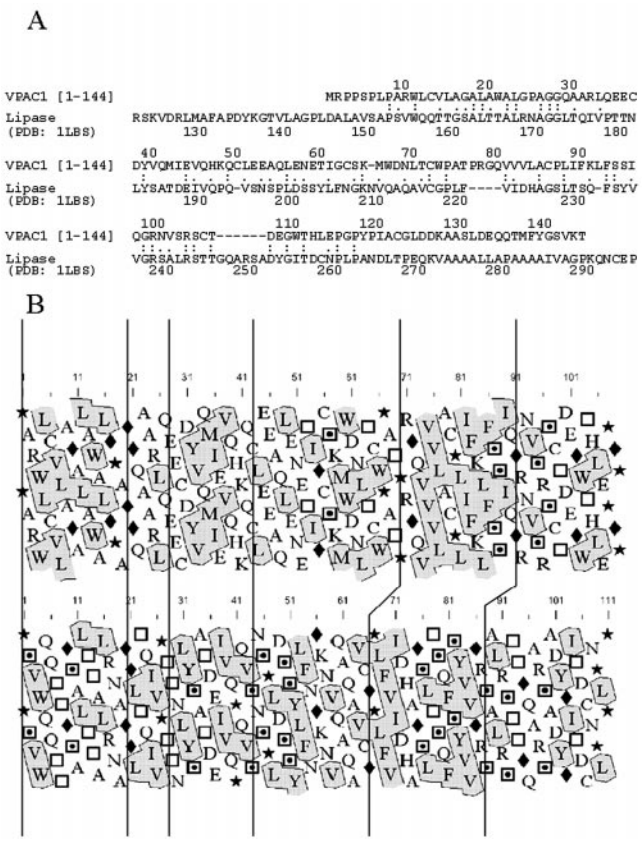

FIG. 1. *A*, sequence alignment between the 1 and 144 domain of human VPAC$_1$ receptor and the 152–262 region of yeast lipase B (PDB code: 1LBS). This alignment was obtained using the FASTA algorithm. *Double dots* and *single dots* indicate amino acid identity and homology in the sequences, respectively. *B*, HCA alignment of the 152–262 domain of yeast lipase B (*upper part*) and the 8–117 N-terminal region of human VPAC$_1$ receptor (*lower part*). ⋆ is Pro, ◆ is Gly, □ is Thr, and ⊡ is Ser. Hydrophobic residues (Leu, Ile, Val, Trp, Tyr, and Phe) are *circled* to delimitate hydrophobic clusters in the protein. *Vertical lines* separate the different hydrophobic clusters that are related in the two proteins.

29% and the β structure represents 7%. This is due to the fact that the lipase subdomain taken as template is poor in α and β structures, with 35 and 9%, respectively.

In previous work (1), we have shown that the N-terminal domain of the human VPAC$_1$ receptor plays an important role in the binding of its natural ligand, VIP. Within the 8–117 region of the receptor, many mutants were previously characterized (7, 8, 11, 13). Five residues, all dispersed along the N-terminal sequence of the VPAC$_1$ receptor are crucial for VIP binding. They include Glu^{36}, Trp^{67}, Asp^{68}, Trp^{73}, and Gly^{109} whose mutation into alanine (7, 11, 13) or glycine (7) or whose deletion (7) completely abolished VIP binding and adenylyl cyclase stimulation (see Table I). All those residues are dispersed in the primary sequence (Fig. 1) but are clearly gathered around a groove in the three-dimensional model (Fig. 3*A*). Conversely, residues whose mutation did not alter the receptor phenotype (see legend to Fig. 3) are randomly mapped in the three-dimensional structure with no preferential localization in the groove (Fig. 3*A*). These observations strongly suggest that the groove is a VIP-binding site of the VPAC$_1$ receptor (Fig. 3*A*). Using CHIME, the electrostatic potential of the three-dimensional model was calculated (Fig. 3*B*). The highly negatively charged nature of the groove (red potential on Fig. 3*B*) reinforces the hypothesis that it could be a VIP-binding site since VIP has several positively charged residues (Arg^{12}, Arg^{14}, Lys^{15}, Lys^{20}, and Lys^{21}). A previous work supported that Arg^{14}, Lys^{15}, and Lys^{21} of VIP directly participate in the binding of the peptide to the human VPAC$_1$ receptor (25). Beside an interesting concentration of charged residues, we also noticed the presence of three tryptophans (Trp^{67}, Trp^{73}, and Trp^{110}) all gathered on top of the electronegative groove (Fig. 4). Two of those residues (Trp^{67} and Trp^{73}) were previously shown to be crucial for the VIP recognition (see Table I). Another interesting feature is the proximity of two Phe residues (Phe^{90} and Phe^{93}) (Fig. 4). Those amino acids could favor II-II interactions with their congeners in VIP (Phe^{6}, Try^{10}, and Tyr^{22}). Indeed, those residues were suggested to be important for VIP structure and/or VIP binding to VPAC$_1$ receptor (25).

To further validate the model, the mutation to alanine of several residues of the negative groove is proposed (Fig. 4). We checked by fluorescence analysis of GFP in living transfected CHO cells that all mutants were expressed in transfected cells as with the wild-type receptor (not shown). The VIP binding parameters (K_d and B_{max}) and the stimulation of adenylyl cyclase activity (EC_{50}) were then measured in stably transfected CHO cells. Table I summarizes the experimental results. To determine the pattern of expression of mutants with null phenotypes (see Table I) in transfected CHO cells, immunofluorescence and antibody binding experiments were performed. Indeed, insertion of a Flag sequence between Ala^{30} and Ala^{31} in the N-terminal extracellular domain of the VPAC$_1$ receptor enabled us to perform indirect immunofluorescence studies and to assess cell surface expression of receptors by anti-Flag antibody binding in nonpermeabilized transfected CHO cells. Microscopy revealed that all mutants studied were delivered at the cell surface like the wild type receptor (Fig. 5). Since immunofluorescence techniques are not quantitative, we also measured cell surface expression of mutants by antibody binding to transfected cells (Table II). It appeared that mutants with null phenotypes did not exhibit any decrease in cell surface expression as compared with that of the wild type receptor. Finally, it should be stated that mutants which exhibit partial activity including P87A and F90A have normal expression since Scatchard analysis of binding data indicated binding capacities similar to that of the wild type receptor (Table I). Several categories of mutants were characterized.

(i) The mutation of the above mentioned aromatic residues including Phe^{90}, Phe^{93}, and Trp^{110} as well as the mutation of Trp^{73} that was previously changed for a glycine were tested. The mutant F90A had a decreased binding affinity for VIP and potency of VIP in stimulating cyclase activity. In contrast, the mutation of F93A did not alter significantly the receptor phenotype supporting that only one aromatic residue (Phe^{90}) would help the binding of VIP. On the other hand, Trp^{73} and Trp^{110} are crucial since the corresponding mutants W73A and W110A exhibit no VIP binding and no VIP-stimulated adenylyl cyclase (Table I). From these data, it can be concluded that all the tryptophan residues located above the electronegative groove are crucial for VIP binding including Trp^{67} (11), Trp^{73}, and Trp^{110} (this paper). They appear to form a shell at one end of the groove (Fig. 6) and could serve different purposes. It could be involved in the structure of the VIP-binding site in the extracellular N-terminal domain of the VPAC$_1$ receptor. This would be in good agreement with the facts that individual mutation of each of the three tryptophans results in a drastic loss of function (see Table I) and that these tryptophans are highly conserved in the class II family of G protein-coupled receptors (1). Since the exposition of the three tryptophans to the water environment is unlikely, they could interact with other domains of the VPAC$_1$ receptor. Alternatively, it could be suggested that the aromatic environment that is formed by the tryptophan shell acts as an anchor for VIP since favorable

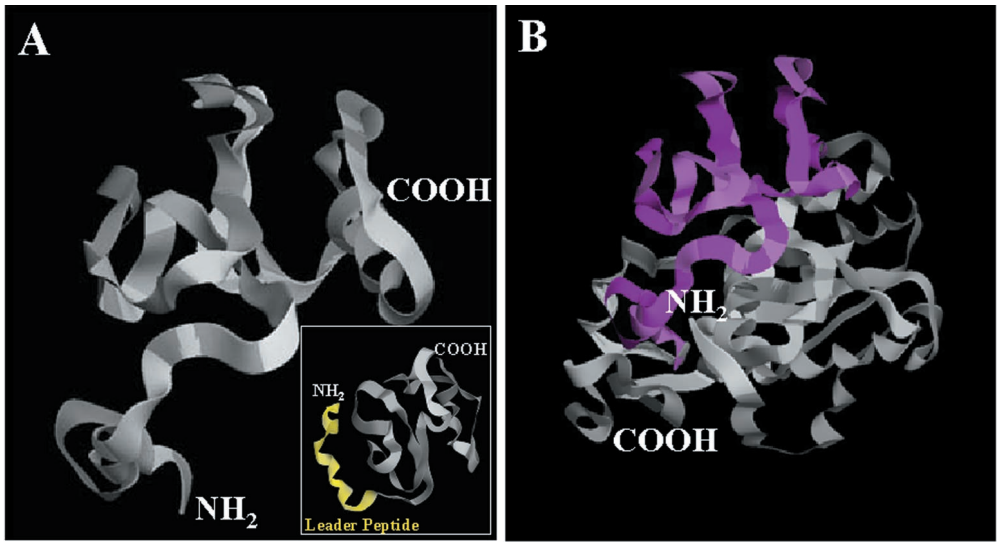

FIG. 2. *A*, ribbon representation of the three-dimensional model of the N-terminal (8–117) domain of the VPAC$_1$ receptor obtained by Modeller 4.0 followed by energy minimization. NH_2 and COOH ends are indicated. *Inset*, same representation rotated by 90° around the *y* axis to highlight the putative N-terminal leader peptide-(8–30) shown in *yellow*. *B,* the three-dimensional structure of the yeast lipase B from the Protein Data Bank (PDB code: 1LBS) is shown for comparison. The region-(152–262) of the lipase which is homologous to the VPAC$_1$-(8–117) receptor domain, is shown in *purple*.

TABLE I

Binding parameters and concentration of VIP eliciting half-maximal stimulation of adenylyl cyclase activity for wild-type human VPAC$_1$ receptor and mutants stably expressed in CHO cells

Dissociation constants (K_d) and binding capacities (B_{max}) were determined by Scatchard analysis of binding data. EC_{50} represents the concentration of VIP giving half-maximal stimulation of adenylyl cyclase. Results are mean ± S.E. of at least three experiments. Previous data regarding the mutants E36A, D68G, W73G, P87G, and Δ109 which are relevant for the present study are described in this table and the corresponding references are cited.

Constructs	K_d	B_{max}	EC_{50}	Refs.
	nM	*fmol/mg of protein*	*nM*	
WT[a]	0.38 ± 0.02	604 ± 23	0.28 ± 0.08	
E36A	—[b]	—	—	13
D38A	0.61 ± 0.15	579 ± 34	1.49 ± 0.64	
K65A	0.74 ± 0.07	835 ± 256	ND[c]	
M66A	—	—	—	
W67A	—	—	—	11
D68G	—	—	ND	7
D68A	—	—	—	
W73G	—	—	ND	7
W73A	—	—	—	
P74A	—	—	—	
R78A	0.40 ± 0.07	352 ± 26	0.77 ± 0.27	
P87G	0.60 ± 0.20	730 ± 120	ND	7
P87A	9.00 ± 0.97	456 ± 43	4.01 ± 0.81	
F90A	3.88 ± 1.77	698 ± 239	3.78 ± 1.03	
K91A	1.13 ± 0.51	640 ± 140	0.37 ± 0.07	
F93A	0.70 ± 0.12	778 ± 92	0.91 ± 0.28	
R99A	0.55 ± 0.21	263 ± 110	0.72 ± 0.18	
E108A	0.60 ± 0.16	600 ± 83	0.23 ± 0.08	
Δ109	—	—	ND	7
G109A	—	—	—	
W110A	—	—	—	

[a] WT, wild-type.
[b] —, binding or enzyme activation not detectable.
[c] ND, not determined.

hydrogen bonding can occur between Trp and aromatic residues (Phe, Tyr, Trp, and His) (30). In the VIP peptide, four residues were previously shown to be important for receptor binding: His^1, Phe^6, Tyr^{10}, and to a lesser extent, Tyr^{22} (25). For aromatic residues present in the N-terminal domain of VIP, especially His^1, this interaction could represent an initial step in the receptor recognition. On this assumption, the N-terminal domain of VIP could initially bind to the groove described herein and then be recognized by a transmembrane binding pocket as suggested by recent data suggesting that Glu^3 of VIP could be in close proximity to transmembrane segment 2 of the VPAC$_1$ receptor (31).

(ii) The model suggests that Pro^{74} and Pro^{87} could be important for the groove structure (Fig. 4). The results demonstrate that the P74A receptor mutant has no detectable binding or stimulation of adenylyl cyclase (Table I). The P87A receptor has a decreased binding affinity for VIP and consequently VIP was less potent to stimulate the cyclase activity (Table I). A previous mutation of Pro^{87} into glycine had no effect on the receptor phenotype (Ref. 7 and Table I). It can be argued that Pro^{87} is less important than Pro^{74} in generating a break in the secondary structure and that its mutation into glycine could accommodate a correct groove structure. This is in line with the fact that proline and glycine are both able to generate breaks in

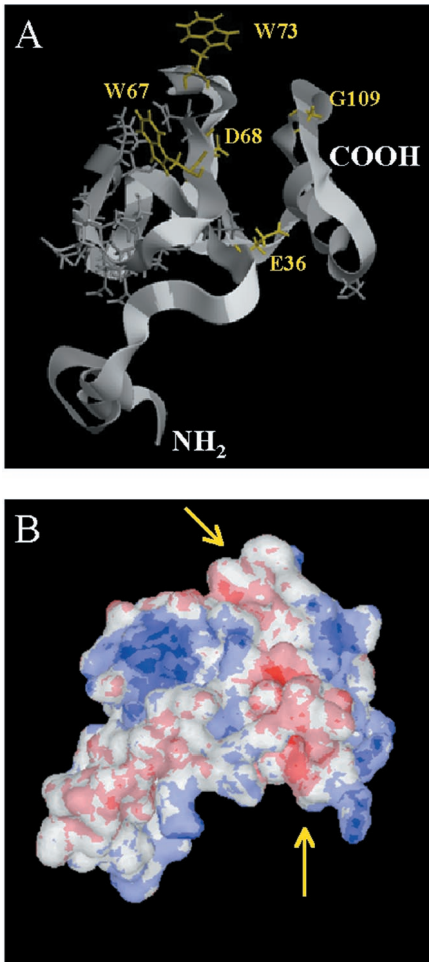

FIG. 3. *A*, ribbon representation of the three-dimensional model of the VPAC$_1$-(8–117) receptor domain showing amino acids which have been previously mutated by directed mutagenesis. *Gray* wireframe represents residues whose mutation into alanine does not change the binding affinity of the VPAC$_1$ receptor for VIP (Gln^{41}, Ile^{43}, Gln^{46}, His^{47}, Lys^{48}, Gln^{49}, Glu^{53}, Gln^{55}, Glu^{57}, Asn^{58}, Glu^{59}, Asn^{69}, and Ser^{102}). *Yellow* wireframe represents amino acids whose mutation into alanine abolishes VIP binding (Glu^{36}, Trp^{67}, Asp^{68}, Trp^{73}, and Gly^{109}). See text and Table I for details. NH$_2$ and COOH ends are indicated. *B*, electrostatic potential on the molecular surface of the three-dimensional model of the VPAC$_1$-(8–117) receptor domain. Colors are: *blue*, positively charged surface; *white*, neutral surface; *red*, negatively charged surface. The *arrows* show the electronegative groove containing the important amino acids described in *A*.

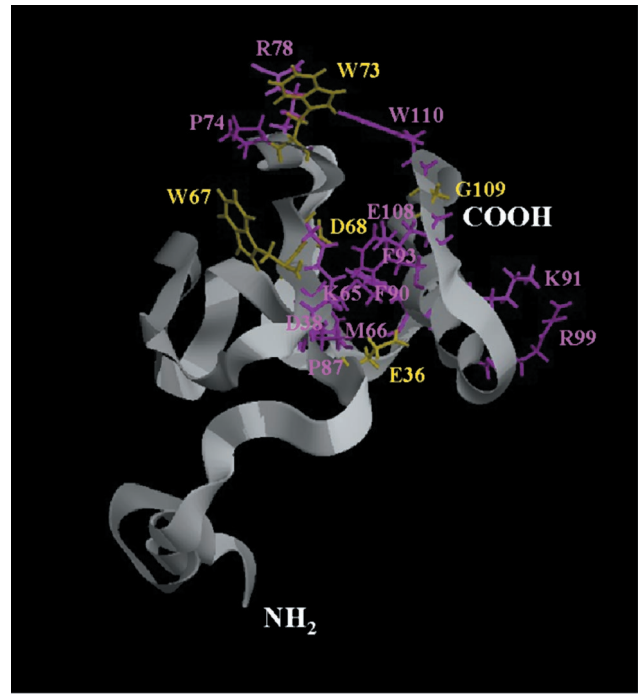

FIG. 4. **Ribbon representation of the three-dimensional model of the VPAC$_1$-(8–117) receptor domain showing amino acids (*purple* wireframe) whose role in VPAC$_1$ receptor function has been tested by site-directed mutagenesis in the present study.** *Yellow* wireframe represents amino acids whose mutation into alanine was previously shown to abolish VIP binding. NH$_2$ and COOH ends are indicated.

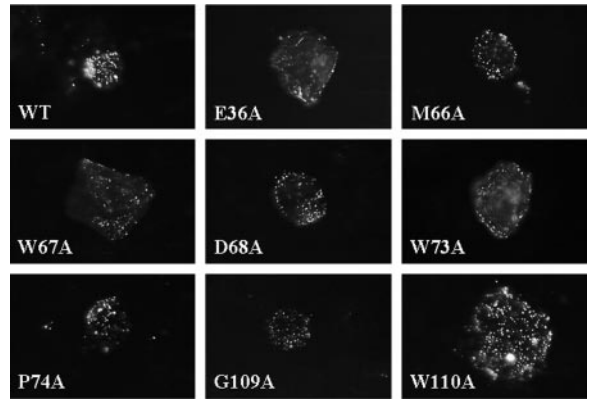

FIG. 5. **Microscopic detection after transfection in CHO cells of the epitope-tagged wild type receptor and receptor mutants with null phenotypes.** Nonpermeabilized cells were incubated with the mouse monoclonal anti-Flag antibodies, washed, incubated with antimouse immunoglobulin G conjugated to rhodamine and pelleted on slides as described under "Experimental Procedures." Controls were carried out with untransfected CHO cells or with CHO cells expressing the epitope-tagged wild type receptor that were incubated only with the rhodamine-labeled antimouse antibody. No fluorescence could be observed in both conditions (not shown).

secondary structures of proteins (32).

(iii) Glu^{36} and Asp^{68}, previously identified as important for VIP binding to its receptor (7, 13), are located in the groove (Fig. 4). While Glu^{36} is rather accessible and available for the interaction with VIP, Asp^{68} appears more deeply buried in the groove. It could be suggested that Asp^{68} which is highly conserved in class II G protein-coupled receptors (7) helps to maintain the structure of the VIP-binding domain possibly through the formation of a salt bridge. The partner of Asp^{68} in this putative salt bridge remains to be determined. On the other hand, one can assume that the docking of VIP should induce dynamically structural reorganization of the groove, such as its opening. Asp^{68} could then be more accessible and interact with one of the positively charged residues of the VIP peptide. During this mechanism, the desolvation energy needed to render Asp^{68} available for an electrostatic interaction with a VIP residue would be greatly decreased as compared with what would be required if Asp^{68} was water-accessible in the groove. Two other negatively charged residues are located in the groove: Asp^{38} and Glu^{108}. While Asp^{38} seems accessible for an interaction with VIP (Fig. 4), the model suggests that the Glu^{108} residue could form a salt bridge with Lys^{65} (mean distance Lys^{65}-Glu^{108}: 4 Å). However, no change of the receptor phenotype was observed with E108A or K65A mutants (Table I) supporting the idea that Glu^{108} and Lys^{65} do not participate in the VIP recognition. These data also suggest that the putative salt bridge between Glu^{108} and Lys^{65} would not be important for maintaining the structure of the VIP-binding site. Neither does expression of D38A support any significant role for Asp^{38} in VIP binding (Table I). This seems contradictory with the idea that the VIP binding occurs in the negative

TABLE II

Cell surface expression of epitope-tagged VPAC1 receptor mutants with null phenotypes after stable transfection of cDNAs into CHO cells

Nonpermeabilized transfected cells were incubated with anti-Flag antibodies and then exposed to the radiolabeled second antibodies. Cells were rinsed, and the radioactivity of cell lysates was counted. Nonspecific binding was determined with cells that were incubated only with the ^{125}I-labeled second antibody. It represented 0.1% of total radioactivity added. Binding of anti-Flag antibodies to epitope-tagged mutant receptors is given as a percentage of anti-Flag antibodies binding to epitope-tagged wild type receptor (mean ± S.E. of three experiments).

Constructs	Surface expression
	% of wild type receptor
WT	100 ± 13
E36A	189 ± 8
M66A	104 ± 23
W67A	130 ± 20
D68A	119 ± 27
W73A	109 ± 17
P74A	137 ± 24
G109A	79 ± 4
W110A	211 ± 60

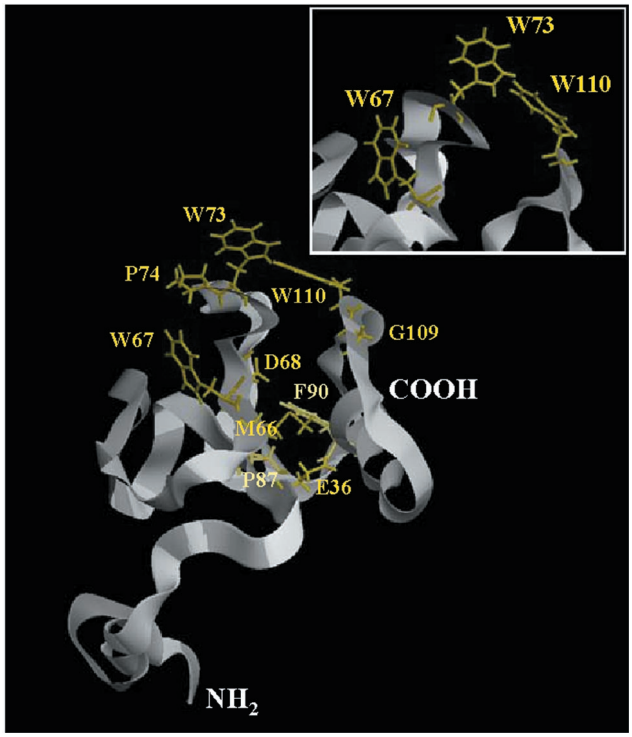

FIG. 6. **Ribbon representation of the three-dimensional model of the VPAC$_1$-(8–117) receptor domain highlighting all amino acids whose mutation alters VIP binding to the VPAC$_1$ receptor.** *Yellow* wireframe represents amino acids whose mutation abolishes VIP binding and *pale yellow* wireframe represents amino acids whose mutation decreases the affinity for VIP (see Table I for experimental data). NH_2 and COOH ends are indicated. *Inset*, three-dimensional representation of the tryptophan shell formed by Trp^{67}, Trp^{73}, and Trp^{110}.

groove. However, a better insight into the model shows that the experimentally crucial negative residues Glu^{36} and Asp^{68} are in the same plane in the groove while Asp^{38} is beneath this plane (Fig. 7). This suggests the existence of a preferential plane of interaction between the VIP and the N-terminal domain of the VPAC$_1$ receptor. Two observations further argue for the existence of this preferential plane. First, the mutation of Met^{66} whose side chain extends in the groove, in the same plane as Glu^{36} and Asp^{68} (Fig. 7) clearly results in a complete loss of VIP binding and adenylyl cyclase activation (Table I).

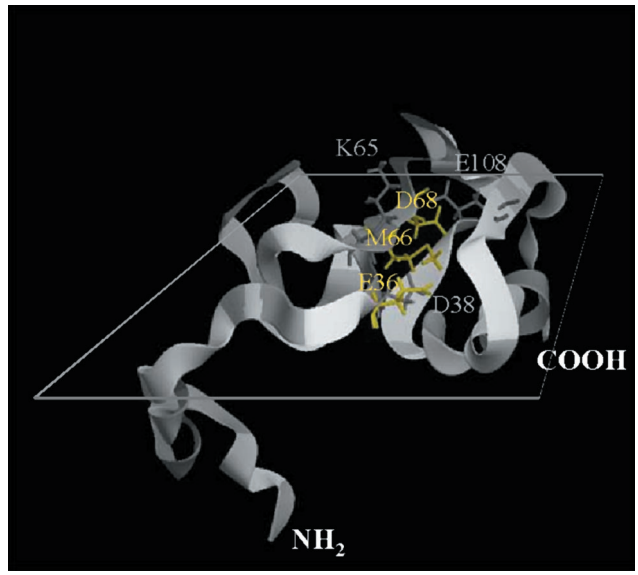

FIG. 7. **Ribbon representation of the three-dimensional model of the VPAC$_1$-(8–117) receptor domain showing Glu^{36}, Met^{66}, and Asp^{68} (*yellow* wireframe) which constitute a putative preferential plane of interaction with VIP.** Other amino acids whose mutation does not alter VIP binding are shown (*gray* wireframe) including Asp^{38} which is below the plane and Glu^{108} (potential salt bridge with Lys^{65}) which is above the plane. NH_2 and COOH ends are indicated.

This highlights the importance of the methionine side chain. Second, a previous study strongly suggested that Arg^{14}, Lys^{15}, and Lys^{21} of VIP are directly participating in the binding of the peptide to the human VPAC$_1$ receptor (25). In the modeled structure of the peptide (25), those residues are almost on the same side of the helix (especially Arg^{14} and Lys^{21}) and their lateral chains point in the same direction. This could suggest that these residues can interact with Glu^{36} and Asp^{68} in the groove. In agreement with this hypothesis is the distance between the Cα of Arg^{14} (and to a lesser extent, Lys^{15}) and the Cα of Lys^{21} in VIP that is approximately 11 Å, equal to the distance between the Cα of Glu^{36} and the Cα of Asp^{68} (Asp ≈ 12 Å) in the VPAC$_1$ receptor.

(iv) Three basic residues Arg^{78}, Lys^{91}, and Arg^{99} are located on the edges of the groove (Lys^{91} and Arg^{99}) or behind the tryptophan shell (Arg^{78}; see Fig. 4). They appear to extend their side chains outside the groove. According to the model they should not be involved in the VIP binding and indeed the mutation of these basic residues did not modify VIP binding (Table I).

(v) Asp^{68} and Gly^{109} (Fig. 4), which are highly conserved in class II G protein-coupled receptors (7), were previously shown to be very important residues for VIP binding on the basis of their deletion or mutation into glycine (7). As a control, D68A and G108A were expressed in this study (Table I). The phenotype of the new mutants confirmed the previous data since a complete loss of VIP binding and adenylyl cyclase activation was observed.

The very good correspondence between the model and the data is especially convincing since the structural model of the VPAC$_1$-(8–117) region was initially generated on a pure sequence homology basis disregarding any of the available experimental data. The model not only clustered all the functionally important residues dispersed in the primary sequence within a groove, but it also pointed out new putatively important residues. We tested those new targets which proved to be involved either in the structure and/or binding function of the VPAC$_1$ receptor. Analysis of the experimental data obtained by site-directed mutagenesis using the model as frame provides the

first comprehensive view of a VIP-binding site of the human VPAC$_1$ receptor and more generally of a peptide-binding domain in the N-terminal extracellular region of the class II family of G protein-coupled receptors. Overall, the data identified a putative binding site (Fig. 6) made of an electronegative groove ending on a tryptophan shell constituted of Trp^{67}, Trp^{73}, and Trp^{110}. Along the groove two acid residues Glu^{36} and Asp^{68} are important. Glu^{36} is not conserved in class II G protein-coupled receptors (13) and could therefore be specific of VIP interaction. Several important basic residues of VIP are candidates for an interaction with Glu^{36} including Arg^{14}, Lys^{15}, and Lys^{21} (25). In contrast, Asp^{68} appears to be more deeply buried in the groove and should be less accessible for a direct interaction with VIP in the current model. A structural role of Asp^{68} by formation of a salt bridge is possible. However, a structural reorganization of the groove in response to the docking of VIP could bring out Asp^{68} for an interaction with the above cited basic residues of VIP.

Other residues could participate in the structure of the VIP binding groove including Pro^{74}, Pro^{87}, and Gly^{109}. The latter residues are highly conserved in class II G protein-coupled receptors (7). Our data also indicate that the side chain of Met^{66} should be accessible in the groove (Figs. 6 and 7). This side chain should be part of a VIP preferential plane of interaction which could be made of the side chains of Glu^{36}, Met^{66}, and potentially Asp^{68}. Indeed the activity of the E36A, D68A, and M66A mutants and the distance between Glu^{36} and Asp^{68} on one hand, and that of Arg^{14} (or Lys^{15}) and Lys^{21} in the VIP peptide, on the other hand, could argue for the existence of such a plane.

Finally, it is important to consider the three consensus *N*-glycosylation sites (Asn^{58}, Asn^{69}, and Asn^{100}). We previously demontrated by site-directed mutagenesis and biochemical experiments that the two sites occupied by a 9-kDa *N*-linked carbohydrate on Asn^{58} or Asn^{69} play a mandatory role for the delivery of the VPAC$_1$ receptor to the plasma membrane (9). In the model, the three asparagines are located at the surface of the structure. The two functionally important glycosylation sites on Asn^{58} and Asn^{69} are clearly accessible to anchor carbohydrates.

The VPAC$_1$ receptor has important cystein residues (1, 8). Six of the eight cysteins present in the N-terminal domain of the receptor are highly conserved in the class II of G protein-coupled receptors. Their mutation abolished VIP binding (8). Five of those cysteins are in the fragment that we modelized. Our model supports that Cys^{72}-Cys^{86} could form a disulfide bridge *in vivo*. Indeed, both residues are mapped at the bottom of the binding groove, facing each other even if they are 12 Å distant (S atom center to S atom center). This distance is longer than the S-S length of a disulfide bridge (2.1 Å). However, it is interesting to note that forcing Cys^{72} and Cys^{86} to reach a distance compatible with a S-S bond (not shown) does not alter the overall structure of the putative VIP binding groove (root mean square deviation between the two models = 1 Å). The other putative S-S bonds cannot be predicted since all functionally important cysteins are not present in the model. For example, the 118–144 domain contains one crucial Cys (Cys^{122}), and the extracellular loops of the transmembrane domain, that are not modelized here, also contain important Cys residues (8, 14).

In line with these restrictions, one must notice that Lys^{143} in the 118–144 domain[2] and Asp^{196} in the first extracellular loop (10) are also clearly important for the VIP binding to the VPAC$_1$ receptor. Therefore, the VIP binding groove we have located in the 8–117 sequence of the receptor by modelization and mutagenesis experiments is most probably a part of the whole VPAC$_1$ receptor-binding site. This is in line with recent data regarding another class II G protein-coupled receptor, the PTH/PTHrP receptor, which highlight the existence of multiple binding subdomains for PTH in the receptor, including an important role for the N-terminal extracellular region of the receptor (33).

In conclusion, structural analysis of the partial three-dimensional model of the VIP-binding site and site-directed mutagenesis reveal that: (i) the N-terminal extremity of the VPAC$_1$ receptor is mostly helical and could correspond to a signal peptide. (ii) The crucial residues for VIP binding and adenylyl cyclase activation by VIP are around a groove containing several negatively charged residues. This groove could be part of the binding site for the VIP which has several positively charged residues. (iii) New residues implied in the VIP recognition and/or structure of the binding groove, suggested from the model (Pro^{74}, Pro^{87}, Phe^{90}, and Trp^{110}) were experimentally validated by site-directed mutagenesis. While the recent report of the three-dimensional crystal structure of rhodopsin at 2.8 Å (34) offers a template for most other G protein-coupled receptors, it does not get the clue to the structure and crucial function of large N-terminal extracellular domains of class II receptors. In this respect, the present work provides the first model of a partial three-dimensional structure of the N-terminal domain of the human VPAC$_1$ receptor and should help to better understand the original structure/function relationship of G-coupled receptors of the class II family.

Acknowledgments—We gratefully acknowledge Dr. Jean-Jacques Lacapère for providing insightful discussions and Dr. Jean-Claude Marie for critical reading of the manuscript.

REFERENCES

1. Laburthe, M., Couvineau, A., Gaudin, P., Rouyer-Fessard, C., Maoret, J. J., and Nicole, P. (1996) *Ann. N. Y. Acad. Sci.* **805,** 94–111
2. Said, S. I. (1991) *Trends Endocrinol. Metab.* **2,** 107–112
3. Gozes, I., Fridkin, M., Hill, J. M., and Brenneman, J. E. (1999) *Curr. Med. Chem.* **6,** 1019–1034
4. Ulrich, C. D., Holtmann, M., and Miller, L. J. (1998) *Gastroenterology* **114,** 382–397
5. Laburthe, M., Couvineau, A., and Voisin, T. (1999) *in Gastrointestinal Endocrinology* (Greeley, G. H., ed) pp. 125–157, Humana Press Inc., Totowa, NJ
6. Segré, G. V., and Goldring, S. R. (1993) *Trends Endocrinol. Metab.* **4,** 309–314
7. Couvineau, A., Gaudin, P., Maoret, J. J., Rouyer-Fessard, C., Nicole, P., and Laburthe, M. (1995) *Biochem. Biophys. Res. Commun.* **206,** 246–252
8. Gaudin, P., Couvineau, A., Maoret, J. J., Rouyer-Fessard, C., and Laburthe, M. (1995) *Biochem. Biophys. Res. Commun.* **211,** 901–908
9. Couvineau, A., Fabre, C., Gaudin, P., Maoret, J. J., and Laburthe, M. (1996) *Biochemistry* **35,** 1745–1752
10. Du, K., Nicole, P., Couvineau, A., and Laburthe, M. (1997) *Biochem. Biophys. Res. Commun.* **230,** 289–292
11. Nicole, P., Maoret, J. J., Couvineau, A., Momany, F. A., and Laburthe, M. (2000) *Biochem. Biophys. Res. Commun.* **276,** 654–659
12. Couvineau, A., Rouyer-Fessard, C., Maoret, J. J., Gaudin, P., Nicole, P., and Laburthe, M. (1996) *J. Biol. Chem.* **271,** 12795–12800
13. Nicole, P., Du, K., Couvineau, A., and Laburthe, M. (1998) *J. Pharmacol. Exp. Ther.* **284,** 744–750
14. Kudsen, S. M., Tams, J. W., Wulff, B. S., and Fahrenkrug, J. (1997) *FEBS Lett.* **412,** 141–143
15. Gaudin, P., Maoret, J. J., Couvineau, A., Rouyer-Fessard, C., and Laburthe, M. (1998) *J. Biol. Chem.* **273,** 4990–4996
16. Gaudin, P., Couvineau, A., Rouyer-Fessard, C., Maoret, J. J., and Laburthe, M. (1999) *Biochem. Biophys. Res. Commun.* **254,** 15–20
17. Laburthe, M., Rousset, M., Rouyer-Fessard, C., Couvineau, A., Chantret, I., Chevalier, G., and Zweibaum, A. (1987) *J. Biol. Chem.* **262,** 10180–10184
18. Sali, A., and Blundell, T. L. (1993) *J. Mol. Biol.* **234,** 779–815
19. Sali, A., Potterton, L., Yuan, F., Van Vlijmen, H., and Karplus, M. (1995) *Proteins Struct. Funct. Genet.* **23,** 318–326
20. Pearson, W. R., and Lipman, D. J. (1988) *Proc. Natl. Acad. Sci. U. S. A.* **85,** 2444–2448
21. Gaboriaud, C., Bissery, V., Benchetrit, T., and Mornon, J. P. (1987) *FEBS Lett.* **224,** 149–155
22. Laskowski, R. A., MacArthur, M. W., Moss, D. S., and Thornton, J. M. (1993) *J. Appl. Cryst.* **26,** 283–291
23. Rahman, M., and Brasseur, R. (1994) *J. Mol. Graph.* **12,** 212–218
24. Couvineau, A., Rouyer-Fessard, C., Darmoul, D., Maoret, J. J., Carrero, I.,

[2] L. Lins, A. Couvineau, C. Rouyer-Fessard, P. Nicole, J-J. Maoret, M. Benhamed, R. Brasseur, A. Thomas, and M. Laburthe, unpublished results.

Ogier-Denis, E., and Laburthe, M. (1994) *Biochem. Biophys. Res. Commun.* **200,** 769–776
25. Nicole, P., Lins, L., Rouyer-Fessard, C., Drouot, C., Fulcrand, P., Thomas, A., Couvineau, A., Martinez, J., Brasseur, R., and Laburthe, M. (2000) *J. Biol. Chem.* **275,** 24003–24012
26. Munson, P. J., and Rodbard, D. (1980) *Anal. Biochem.* **197,** 220–239
27. Laburthe, M., Couvineau, A., and Rouyer-Fessard, C. (1986) *Mol. Pharmacol.* **29,** 23–27
28. Bradford, M. M. (1979) *Anal. Biochem.* **78,** 248–254
29. Orengo, C. A., Michie, A. D., Jones, D. T., Swindells, M. B., and Thornton, J. M. (1997) *Structure* **5,** 1093–1108
30. Nishio, M., Hirota, M., and Umezawa, Y. (1998) in *The CH/*Π *Interaction* (Marchand, P. A., ed) pp. 175–202, Wiley-VCH, New York
31. Solano, R. M., Langer, I., Perret, J., Vertongen, P., Juarranz, M. G., Robberecht, P., and Waelbroeck, M. (2001) *J. Biol. Chem*. **276,** 1084–1088
32. Chou, P. Y., and Fasman, G. D. (1977) *J. Mol. Biol.* **115,** 135–175
33. Jin, L., Briggs, S. L., Chandrasekhar, S., Chirgadze, N. Y., Clawson, D. K., Schevitz, R. W., Smiley, D. L., Tashjian, A. H., and Zhang, F. (2000) *J. Biol. Chem.* **275,** 27238–27244
34. Palcewski, K., Kumasaka, T., Hori, T., Behnke, C. A., Motoshima, H., Fox, B. A., Le Trong, I., Teller, D. C., Okada, T., Stenkamp, R. E., Yamamoto, M., and Miyano, M. (2000) *Science* **289,** 739–745